Preparation and Characterization of Low Density Polyethylene/Ethylene Methyl Acrylate Glycidyl Methacrylate/Organoclay Nanocomposites

Fatma Isik Coskunses, Ulku Yilmazer

Chemical Engineering Department, Middle East Technical University, 06531 Ankara, Turkey

Received 21 May 2010; accepted 2 October 2010
DOI 10.1002/app.33482
Published online 12 January 2011 in Wiley Online Library (wileyonlinelibrary.com).

ABSTRACT: The effects of organoclay type, compatibilizer, and the addition order of components during melt-blending process on the morphology and thermal, mechanical, and flow properties of ternary nanocomposites based on low-density polyethylene (LDPE) were investigated. As a compatibilizer, ethylene/methyl acrylate/glycidyl methacrylate (E-MA-GMA), as organoclays Cloisites® 15A, 25A, and 30B were used. All samples were prepared by a corotating twin screw extruder, followed by injection molding. The highest increase of the basal spacing for ternary nanocomposites was obtained in LDPE/E-MA-GMA/Cloisite® 30B nanocomposites with interlayer spacing of 59.2 Å. Organoclay and compatibilizer addition did not influence the melting/crystallization behavior of the compositions, and both compatibilizer and organoclays had no significant nucleation activity in LDPE. Among the ternary nanocomposites, the maximum increase in tensile strength and tensile modulus values was observed for nanocomposites containing organoclay Cloisite® 15A. The improvement with respect to neat LDPE was 43% for tensile strength and 44% for tensile modulus. According to the mechanical analysis, the best sequence of component addition was the one in which LDPE, organoclay, and compatibilizer were simultaneously fed to the extruder in the first run, and the product of the first run was extruded once more. © 2011 Wiley Periodicals, Inc. J Appl Polym Sci 120: 3087–3097, 2011

Key words: low-density polyethylene; compatibilizer; organoclay; nanocomposite; ethylene/methyl acrylate/glycidyl methacrylate

INTRODUCTION

Nanocomposites are a special class of composites, containing fillers, at least one dimension of which is in the nanometer (10^{-9} m) range.[1] Owing to the structural properties gained by well dispersion of the nanosized fillers, nanocomposites possess highly improved mechanical, thermal, physical, and barrier properties when compared with pristine polymer and conventional composites.[2] Among the inorganic fillers, layered silicates are the most widely used reinforcements in nanocomposites owing to their high-aspect ratio. If the silicate layers are well dispersed throughout the polymer matrix, interaction of the filler and polymer significantly increases, and the properties of the matrix material are improved.

Montmorillonite, which belongs to the general family of 2 : 1-layered silicates, is the most commonly used smectite clay in nanocomposites. The structure of montmorillonite consists of an octahedral alumina sheet between two tetrahedral silica sheets. The layer thickness of the crystal structure is around 1 nm, and the lateral dimensions of these layers may be in the range of 30 nm to several microns or larger.[3] Natural montmorillonite is hydrophilic; thus, it is incompatible with many hydrophobic engineering polymers, because the layered silicates are not easily dispersed in most polymers. To overcome this problem, a simple cation exchange process is applied to montmorillonite to make the clay organophilic.

Organoclay–polyethylene nanocomposites prepared by melt compounding have been of interest.[4–15] Wang et al.[8] produced maleated polyethylene/clay nanocomposites and indicated that the hydrophobicity of the organically modified clay and the hydrophilicity of maleated polyethylene are important factors to obtain exfoliated and homogeneously dispersed clay nanocomposites. Zhang et al.[9] studied flammability properties of polyethylene–clay nanocomposites and found that there is considerable reduction in the peak release rate in the nanocomposites. It was also observed that polyethylene–clay nanocomposites have a mixed immiscible-intercalated structure, and there is better intercalation when maleic anhydride is combined with the polymer and clay.[9] Incompatibility of organoclay and polyethylene, which is nonpolar, brings out the necessity of using a compatibilizer in nanocomposite production. Significant increase in

Correspondence to: U. Yilmazer (yilmazer@metu.edu.tr).
Contract grant sponsor: Middle East Technical University; contract grant number: BAP-2005-07-02-00-66.

thermal and mechanical properties and dispersion of clay in polyolefin/organoclay nanocomposites was obtained by the addition of compatibilizer in several studies.[10–14] Liang et al.[10] prepared ternary nanocomposites by two blending processes; direct melt blending and solution blending. Maleic anhydride-grafted HDPE and LDPE and organic montmorillonite were used in their study. It was shown that organic montmorillonite and PE-*g*-MA have a heterogeneous nucleation effect on crystallization of PE from the melt. Hotta and coworkers[11] prepared linear low-density polyethylene (LLDPE)/organoclay nanocomposites by melt-compounding method and studied the effect of the number of alkyl groups of organoclay on exfoliation and the improvement of mechanical properties for LLDPE-clay nanocomposites prepared with and without LLDPE-*g*-MA. It was concluded that, nanocomposites prepared with organoclay having two alkyl tails have better properties in terms of clay dispersion and mechanical properties. Morawiec et al.[12] obtained LDPE nanocomposites with organo-modified clay and anhydride-grafted LDPE. Thermal and mechanical properties of the neat LDPE were improved, and it was shown that the improvement in the mechanical properties was achieved not only by the clay exfoliation and clay content, but also by the addition of a significant amount of the compatibilizer. Hwang et al.[13] worked on the effects of organoclay and compatibilizer, LDPE-*g*-MA, on the mechanical and thermal properties of the injection-molded LDPE microcellular nanocomposites. In the study of Yang et al.[14] ethylene vinyl acetate copolymer was used as compatibilizer for LDPE/organoclay (MMT) nanocomposites, and exfoliated structures were obtained by using a two-step melt-compounding technique.

The objective of this study is to investigate the effects of compatibilizer, organoclay type, and the addition order of the components on the properties of LDPE-compatibilizer-organoclay ternary nanocomposites. The compatibilizer used was a terpolymer of ethylene/methyl acrylate/glycidyl methacrylate (E-MA-GMA), and the organoclays used were Cloisites® 15A, 25A, and 30B. This compatibilizer has not been used in LDPE-organoclay nanocomposites, and it produces significant improvements in dispersion and mechanical properties as discussed later on.

EXPERIMENTAL

Materials

LDPE, Petilen G03-5 with density 0.920 g/cm^3 was supplied by Petkim Petrokimya Holding A.Ş, Izmir, Turkey. Three different natural montmorillonites: Cloisites® 15A, 25A, and 30B modified with various quaternary ammonium salts were purchased from Southern Clay Products, TX. The cation of the organic modifier of Cloisite® 15A is dimethyl, dehydrogenated tallow quaternary ammonium (2M2HT) with a concentration of 125 mEq/100 g clay, and the anion is chloride. Cloisite® 25A is an organoclay modified by the cation dimethyl, dehydrogenated tallow, 2-ethylhexyl quaternary ammonium (2MHTL8) at a concentration of 95 mEq/100 g clay, and the anion is methyl sulfate. The cation of the organic modifier of Cloisite® 30B is methyl, tallow, *bis*-2-hydroxyethyl, quaternary ammonium (MT2EtOH) at a concentration of 90 mEq/100 g clay, and the anion is chloride.

The compatibilizer, a terpolymer of E-MA-GMA, was purchased from Arkema, France. The trade name of the compatibilizer is Lotader® AX8900 (MFI = 6 g/10 min, at 190°C, 2.16 kg).

TABLE I
Drying Conditions of Materials

Materials	Drying temperature (°C)	Drying time (h)
Before RUN I extrusion process		
LDPE	–	–
E-MA-GMA	40	12–15
Cloisite® 15A	120	12–15
Cloisite® 25A		
Cloisite® 30B		
Before RUN II extrusion process		
LDPE	100	4
LDPE/E-MA-GMA	100	4
LDPE/Clay	100	4
E-MA-GMA/Clay	40	4
LDPE/E-MA-GMA/Clay	100	4
Before injection-molding process		
All samples	100	12–15

Nanocomposite preparation

Ternary nanocomposites of LDPE/E-MA-GMA/organoclay, having 5 wt % compatibilizer and 2 wt % organoclay, were produced in pellet form by a two-step extrusion process using a corotating twin-screw extruder. The extruder used was Thermoprism TSE 16 TC with $L/D = 24$, barrel length of 384 mm and die length of 16 mm. During the extrusion process, the temperature profile, the screw speed, and the total flow rate of feed were constant in all the experiments. Process temperatures were 170, 210, 210, 210, and 220°C for the hopper, the three mixing zones, and the die, respectively. The screw speed and total flow rate of feed were 200 rpm and 25 g/min throughout the experiments. Before each run of extrusion process, the raw materials and precompounded samples were dried to get rid of the moisture. The drying conditions are given in Table I. There is no risk of degradation of the polymers and the organoclays under these drying conditions.

TABLE II
Addition Order Procedures of Melt Blending

	RUN I		RUN II	
Addition order	Main-feeder	Side-feeder	Main-feeder	Side-feeder
AO1 (CoC)-P	E-MA-GMA	Cloisite® 15A	Product of Run I + LDPE	–
AO2 (PC)-Co	LDPE	Cloisite® 15A	Product of Run I + E-MA-GMA	–
AO3 (PCo)-C	LDPE	E-MA-GMA	Product of Run I	Cloisite® 15A
AO4 (PCoC)	LDPE /E-MA-GMA	Cloisite® 15A	Product of Run I	–

LDPE, E-MA-GMA, and pelletized form of first run extrusion products were fed to the extruder through the main feeder, and the organoclay was fed through the side feeder. The molten product obtained from the extruder barrel was cooled by passing through a water bath, whose temperature was continuously controlled. At the end of the water bath, an air fan was placed to remove the water from the product surface, and, finally, the product was collected after passing through the pelletizer.

Binary mixtures of LDPE/organoclay and LDPE/E-MA-GMA were also prepared under the same process conditions to compare with the properties of ternary nanocomposites and determine the effects of organoclay and compatibilizer on the properties of the nanocomposites. Neat LDPE was also extruded twice, so that it undergoes similar process history.

Addition order of raw materials

Four different addition order procedures were applied to produce LDPE/E-MA-GMA/ Cloisite® 15A nanocomposites with 2 wt % Cloisite® 15A and 5 wt % E-MA-GMA. All nanocomposites were produced by using a two-step melt-compounding procedure with a twin-screw extruder, namely Run I and Run II. Table II summarizes the four different addition procedures of the raw materials. They can be summarized as follows:

$$\text{AO1} = [\text{Co C}]\text{P};\ \text{AO2} = [\text{P C}]\text{Co};$$
$$\text{AO3} = [\text{P Co}]\text{C};\ \text{AO4} = [\text{P Co C}]$$

where P, Co, and C refer to polymer (LDPE), compatibilizer (E-MA-GMA), and clay (Cloisite®), respectively. The parenthesis denotes the first run of the extrusions. In the second run of the extrusion process, the third material was added to the system.

Characterization experiment

The specimens for morphological, thermal, and mechanical characterization were obtained by using a laboratory scale injection-molding machine (Daca Instruments). The nozzle temperature and mold temperature were 220°C and 30°C, respectively.

The samples containing organoclay were analyzed with a Philips PW3710-based X-Ray diffractometer. Cu-K anode radiation, generated at a generator tension of 40 kV and current of 55 mA, was used as the X-ray source. The diffraction patterns were collected in the diffraction angle, 2θ, range of 1°–10° at a scanning rate, and step size of 3°/min and 0.02°, respectively.

The morphology and structure of the layered silicates were examined by means of scanning as well as transmission electron microscopy. Scanning electron microscopy was performed by a JEOL JSM-6400 low-voltage scanning electron microscope. The fractured surfaces were obtained by immersing the samples in liquid nitrogen, followed by impact. Philips CM200 Transmission Electron Microscope at an acceleralation voltage of 120 kV was used to examine the samples by TEM. All samples were trimmed parallel to the injection-molding direction. Ultrathin sections of 70 nm in thickness were cryogenically cut with a diamond knife at a temperature of −100°C.

Thermal characterization was performed, by using a differential scanning calorimeter, General V4.1.C DuPont 2000 on samples that were cut from injection-molded samples used in mechanical property evaluation. Measurements were carried out in the temperature range of 30–180°C, with a heating rate of 10°C/min under nitrogen atmosphere. First run results are reported to correlate the DSC results with the mechanical properties determined on injection-molded samples. Melting points of samples and the degree of crystallinity were determined. The amount of inorganic additives was taken into account in determining the crystallinity. The heat of fusion (ΔH) value for 100% crystalline LDPE was taken as 293 J/g.[12]

Tensile tests were performed for each composition according to the procedure identified in ASTM D638M-91a (Standard Test Method for Tensile Properties of Plastics),[15] by using a Lloyd LR 30 K Universal Testing Machine. The properties were reported as the average of the results of five samples. Melt flow index (MFI) tests were performed according to ASTM D1238-79 procedure using an Omega Melt Flow Indexer. The measurements were carried out at 270°C with a load of 2.16 kg, and the results were reported in g/10 min. It should be noted that

this temperature is significantly higher than the temperature of 190°C used in industry for polyethylene.

RESULTS AND DISCUSSION

Morphological characterization of nanocomposites

Three complementary techniques, XRD, SEM, and TEM analysis, were performed to characterize the morphology of the nanocomposites.

X-ray diffraction analysis

Interlayer spacing of the silicate layers was determined using the peak positions according to Bragg's law: $d = \lambda n/(2 \sin \theta)$. The XRD data of the neat organoclays, LDPE/organoclay binary nanocomposites, and LDPE/E-MA-GMA/organoclay ternary nanocomposites are shown in Figures 1–3. The intensity values are shifted for clarity.

The basal spacing of neat organoclays was determined as 31.9 Å, 20.1 Å, and 17.9 Å for Cloisites® 15A, 25A, and 30B, respectively, and these values are in accordance with the values of basal spacings reported in the manufacturer's data sheet. Cloisite® 15A organoclay has two peaks as shown in Figure 1. The peak at 12.8 Å corresponds to unintercalated clay.

Among the binary nanocomposites of LDPE/organoclays, intercalated structure was obtained in the material containing 2 wt % Cloisite® 25A shown in Figure 2. The binary composite had a peak at 3.09° in the XRD pattern, indicating a basal spacing of 28.5 Å. In the XRD pattern, there was also another broader peak with basal spacing of 16.4 Å, which could be due to the unintercalated layers. Note that the original basal spacing of Cloisite® 25A in powder form was shown by a broad peak at 20.1 Å. The peaks at *d*-spacing values smaller than the neat organoclay's basal spacing belong to the unintercalated organoclay. During the melt-blending process, the alkyl chains of the organoclay get rearranged, and breakup of the electrostatic interaction between the alkyl ammonium and the negative charge of the silicate surface may result in decrease in the basal spacing.[16]

The interlamellar distances of silicate layers of the organoclay Cloisite® 15A shown in Figure 1 increased slightly upon compounding with LDPE. The peak at 12.8 Å was shifted to 17.7 Å, while the peak at 31.9 Å was shifted to 33.3 Å as shown in Figure 1(b). In the case of Cloisite® 30B shown in

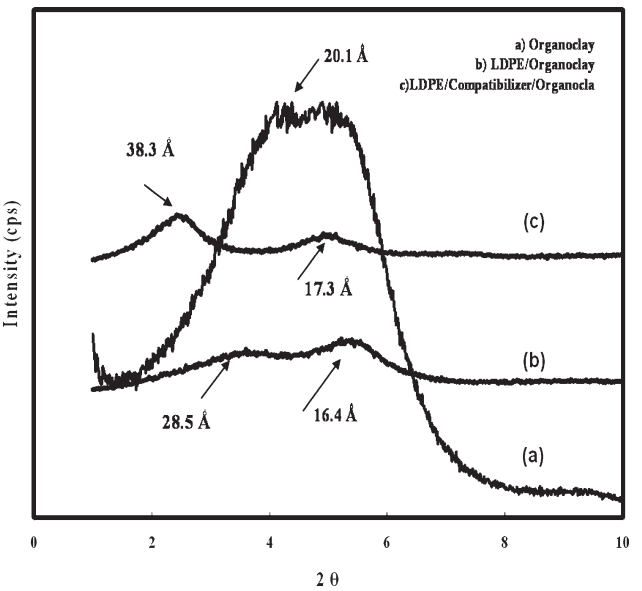

Figure 2 XRD patterns for (a) Cloisite® 25A, (b) LDPE/Cloisite® 25A, and (c) LDPE/E-MA-GMA/Cloisite® 25A.

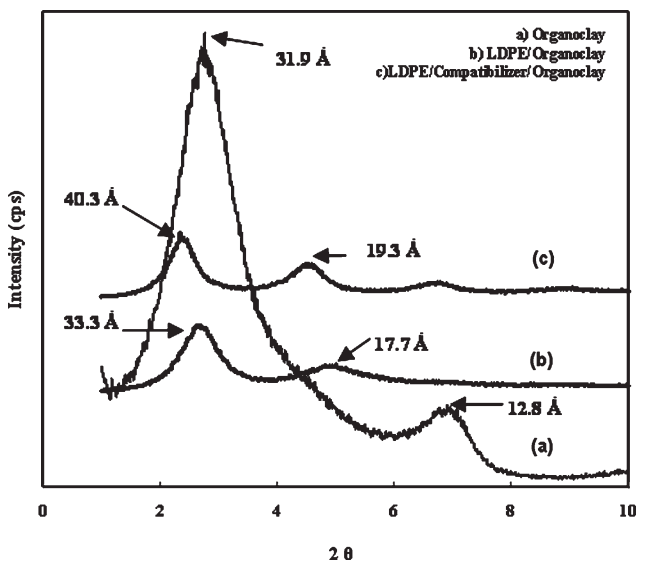

Figure 1 XRD patterns for (a) Cloisite® 15A, (b) LDPE/Cloisite® 15A, and (c) LDPE/E-MA-GMA/Cloisite® 15A.

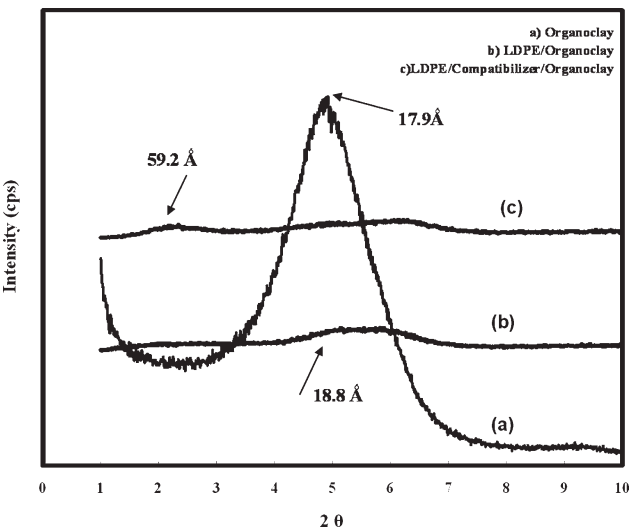

Figure 3 XRD patterns for (a) Cloisite® 30B, (b) LDPE/Cloisite® 30B, and (c) LDPE/E-MA-GMA/Cloisite® 30B.

Figure 3, the peak at 17.9 Å was shifted to 18.8 Å. Especially, in Cloisite® 30B, the peak height of the binary nanocomposite was very small, indicating an intercalated/exfoliated structure.

Effect of compatibilizer

The alkyl chains of organoclays provide an additional distance between the interlayer of the layered silicates making it easier for the polymer matrix to enter into the clay galleries. As shown in Figures 1–3, addition of 5 wt % compatibilizer to the LDPE/organoclay nanocomposites resulted in shifting of the characteristic diffraction peaks of the neat organoclay and LDPE/organoclay binary nanocomposites to smaller angles, indicating higher interlayer spacing of the clay layers. In the diffractograms of the nanocomposites, secondary peaks were also observed. This shows that there are several intercalated structures with different basal spacings, which were formed during the insertion of the polymer into the clay galleries and resulted in more disordered structures.[17]

Considering the ternary LDPE/E-MA-GMA/organoclay nanocomposites, the one with Cloisite® 15A shown in Figure 1 with (c) has a diffraction peak at angle 2.19° corresponding to an interlayer spacing of 40.3 Å. This peak implies that insertion of polymer chains caused intercalation, but complete exfoliation was not achieved. In Figure 2, XRD pattern of the ternary nanocomposite containing Cloisite® 25A showed peaks with basal spacings of 38.3 Å and 17.3 Å, indicating that this nanocomposite also has an intercalated structure. Among all the compositions, the best dispersion was achieved with Cloisite® 30B. The interlayer spacing was determined as 59.2 Å, and the height of the peak was lower in comparison with others, indicating a highly exfoliated/intercalated structure.

E-MA-GMA is polyethylene based; therefore, it is highly miscible with the polyethylene matrix of the nanocomposites, and it also contains the functional group of GMA. It can react with the hydroxyl groups of the montmorillonite and the organoclay Cloisite® 30B. This results in the intercalation of the compatibilizer into the clay galleries and increases the possibility of the delamination of the clay structure. The presence of bulky functional groups such as MA and GMA also increases the clay spacing and decreases the interaction between the clay layers, thus enhancing intercalation and exfoliation.

Effect of addition order

X-ray diffraction analysis was performed for LDPE/E-MA-GMA/Cloisite® 15A nanocomposites containing 5 wt % compatibilizer and 2 wt % Cloisite® 15A, obtained through different addition order procedures during melt blending. The XRD results are given in Figure 4. The affect of the addition order was studied for Cloisite® 15A, because, as shown later, the highest improvements in mechanical properties were obtained in nanocomposites with Cloisite® 15A.

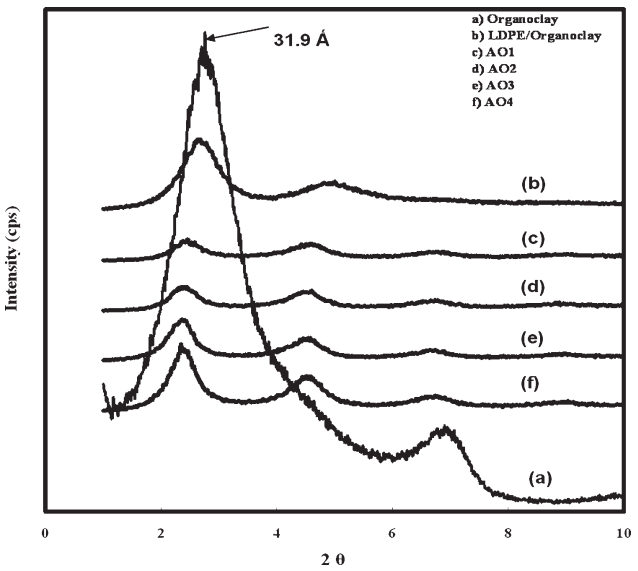

Figure 4 (a) Cloisite® 15A, (b) LDPE/Cloisite® 15A, (c) AO1 (CoC)-P, (d) AO2 (PC)-Co, (e) AO3 (PCo)-C, and (f) AO4 (PCoC).

Considering the LDPE/E-MA-GMA/Cloisite® 15A nanocomposites, the peak of montmorillonite apparently shifts to a smaller angle in all the addition order sequences. All samples have diffraction peaks corresponding to basal spacing of 40.8 Å, indicating that intercalated nanocomposites were obtained.

SEM and TEM analysis

Figure 5 shows the fractured surface of twice extruded LDPE at magnification of ×3000. LDPE has a smooth surface and few crack propagation lines. These are mostly straight propagation lines and due to the homogeneous structure, there are no significant barriers to stop the crack propagation. The collinear position of crack lines enhances crack growth, and so it is possible to obtain fracture with only small amounts of energy.[18] It is observed that addition of organoclay to the polymer matrix had resulted in an obvious change in the morphology of the neat polymer matrix. Figure 6 is the micrograph of LDPE/organoclay binary composition with 2 wt % Cloisite® 25A. In Figure 6, the crack propagation lines are shorter and closer, and instead of being straight lines, they are more zigzagged and tortuous. These tortuous paths prevent easy propagation of the cracks. Generally, as the distance between the crack lines is smaller, the material can

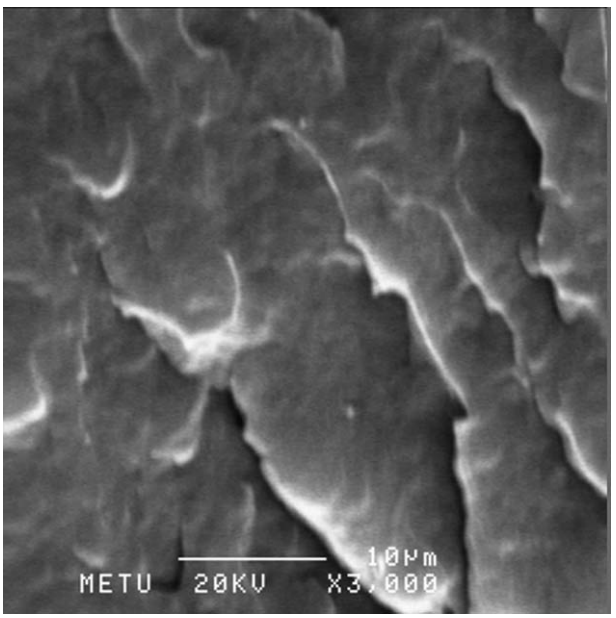

Figure 5 SEM micrograph of pure LDPE.

endure higher impact stresses. Figure 7 is the micrograph of LDPE/E-MA-GMA blend with 5 wt % E-MA-GMA. It is very similar to Figure 5, which belongs to the neat LDPE. This similarity and the continuous and interpenetrated phases seen in the micrograph indicate that the compatibilizer E-MA-GMA is compatible with LDPE. Figure 8 is the SEM micrograph of the fractured surfaces of ternary LDPE/E-MA-GMA/Cloisite® 15A nanocomposite containing 5 wt % E-MA-GMA and 2 wt % Cloisite® 15A prepared by the fourth addition sequence (PCoC), in which all the materials were fed to

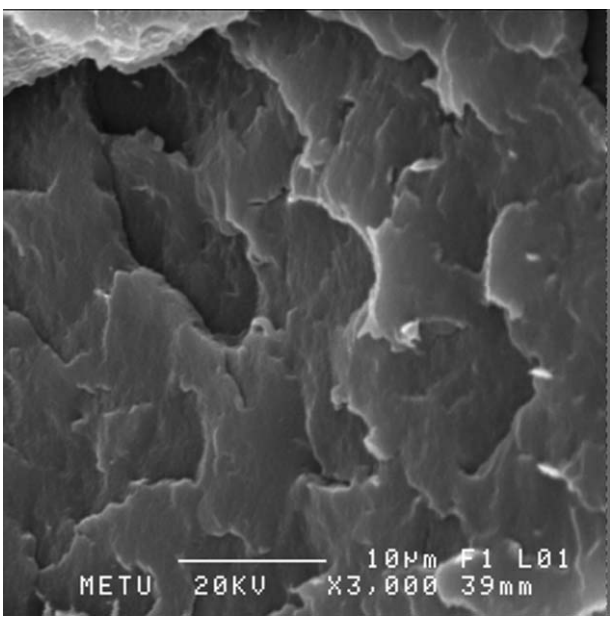

Figure 6 SEM micrograph of binary LDPE/organoclay nanocomposite containing 2 wt % Cloisite® 25A.

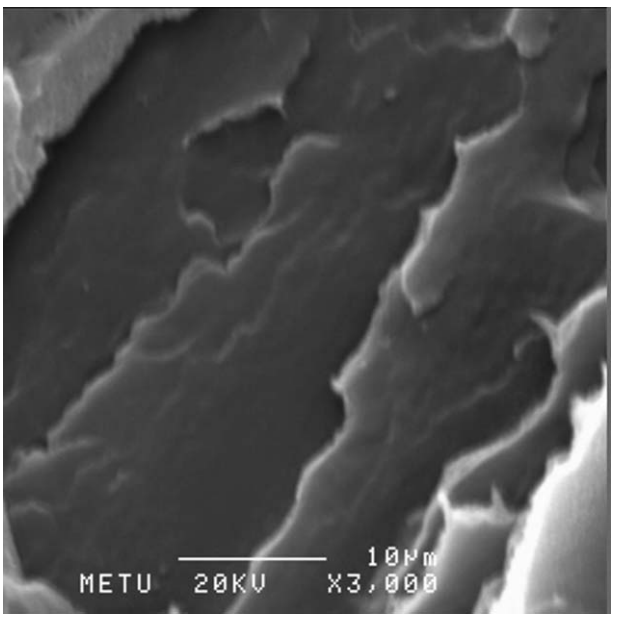

Figure 7 SEM micrograph of binary LDPE/compatibilizer blend containing 5 wt % E-MA-GMA.

extruder simultaneously in the first run, and the product of the first run was extruded once more. The crack propagation lines of nanocomposite surfaces are not straight lines, and the smooth structure of neat LDPE is not detected in these SEM micrographs. In the case of well-dispersed layered silicates, many shorter and closer, circular, nonlinear, and cracks are formed, and these nonlinear cracks tend to grow until they interfere with each other. At

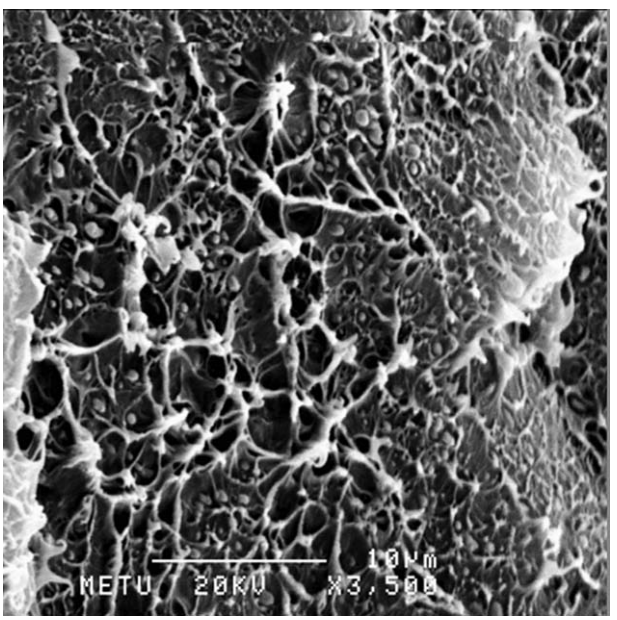

Figure 8 SEM micrograph of ternary LDPE/E-MA-GMA/organoclay nanocomposite containing 5 wt % E-MA-GMA and 2 wt % Cloisite® 15A, prepared by the fourth addition order sequence.

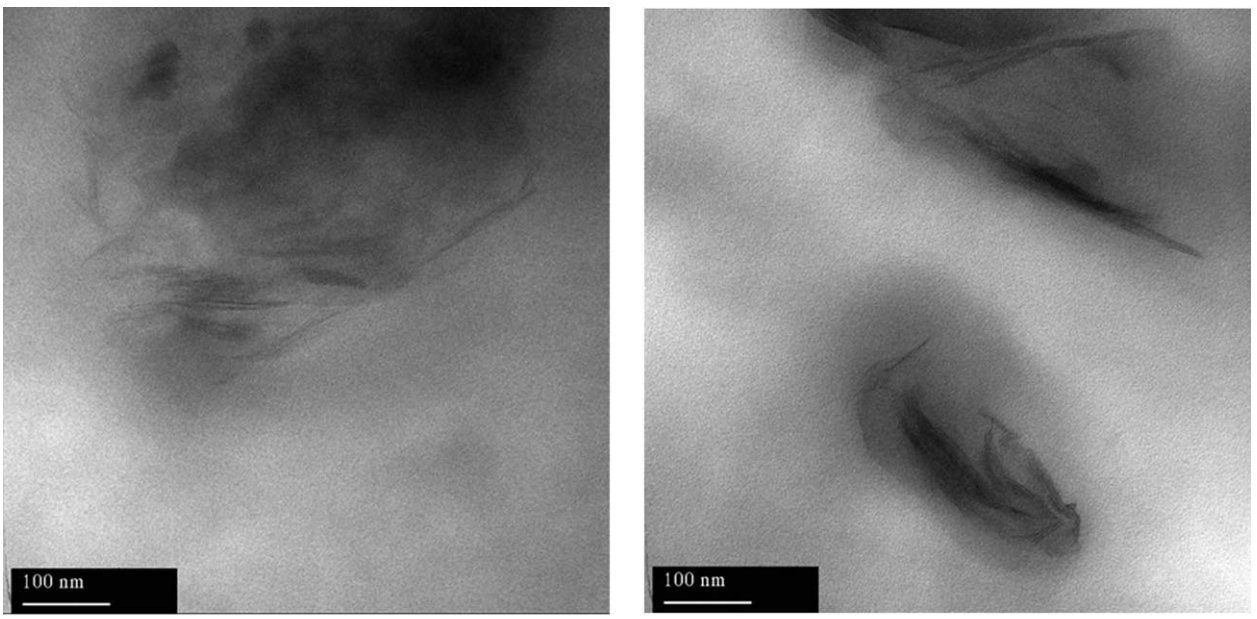

Figure 9 (a) TEM micrograph of ternary LDPE/E-MA-GMA/organoclay nanocomposite containing 5 wt % E-MA-GMA and 2 wt % Cloisite® 15A, prepared by the fourth addition order sequence. (b) TEM micrograph of ternary LDPE/E-MA-GMA/organoclay nanocomposite containing 5 wt % E-MA-GMA and 2 wt % Cloisite® 15A, prepared by the fourth addition order sequence.

these points, the stress fields at the tips of the crack lines interact and prevent further growth of cracks by reducing the stress at the tips of the cracks.[18] When compared with SEM micrographs of LDPE/organoclay binary nanocomposites, addition of compatibilizer resulted in more tortuous crack propagation lines in comparison with those of the binary nanocomposites. The improved mechanical properties of the ternary nanocomposites and XRD results also support the compatibility of the phases and well dispersion of the clay particles in the ternary nanocomposites.

The SEM micrographs of ternary nanocomposites prepared by different addition order procedures (not shown here) indicated no significant differences in the morphology of the fractured surfaces. All the surfaces were highly rough, and the crack propagation lines were tortuous as in Figure 8.

Figure 9(a,b) is the TEM micrographs of LDPE/E-MA-GMA/organoclay nanocomposites containing 5 wt % E-MA-GMA and 2 wt % Cloisite® 15A. TEM images help to obtain a better observation of the nanostructures, owing to the high resolution of the analysis method. The gray areas in the figures are the polymer/compatibilizer matrix, and the black regions are the organoclay structures in the form of individual silicate layers and their agglomerates (tactoids). Figure 9(a,b) confirms that compatibilized polymer matrix had intercalated into the layers of Cloisite® 15A, and intercalation of the clay platelets was achieved. These observations are in accordance with the results of the XRD analysis.

Thermal characterization of the nanocomposites

To investigate the effects of the organoclay and compatibilizer on the thermal properties of nanocomposites in terms of melting temperature and crystallinity, DSC analysis were performed to neat LDPE, binary nanocomposites of LDPE/organoclay, and also the ternary compositions of LDPE/2 wt % organoclay/5 wt % compatibilizer. The results of the DSC are shown in Table III. The glass transition temperature of the LDPE and the compatibilizers are below the room temperature, thus it was not detected in this DSC analysis. The melting point of the compatibilizer E-MA-GMA is reported as 60°C in manufacturer's data sheet. During the calculations, the heat of fusion (ΔH) value for 100% crystalline LDPE was taken as 293 J/g.[12] There were no significant changes in the melting point and % crystallinity of samples. The variation of melting point was only 1–2°C, suggesting that the addition of organoclay and compatibilizer does not significantly influence the melting/crystallization behavior of the compositions. As far as the crystallinity of the materials, DSC results did not show any remarkable differences between the samples. Thus, it was concluded that, both E-MA-GMA and organoclays have no significant nucleation activity in LDPE.

TABLE III
DSC Analysis Results of Samples Containing 5 wt % Compatibilizer, 2 wt % Organoclay

Composition	ΔH (J/g)	LDPE (wt %)	% crystallinity	T_m (°C)
LDPE (neat polymer)	79.47	100	0.27	112.18
LDPE/Cloisite® 15A	79.65	98	0.28	111.71
LDPE/Cloisite® 25A	79.05	98	0.28	111.86
LDPE/Cloisite® 30B	83.46	98	0.29	112.43
LDPE/E-MA-GMA	83.24	95	0.30	110.88
LDPE/E-MA-GMA/Cloisite® 15A	73.13	93	0.27	112.11

Mechanical characterization of nanocomposites

Tensile properties

The tensile properties including tensile strength, tensile modulus, and tensile strain at break value of all the compositions prepared in this study, together with the values of corresponding neat polymer were evaluated, and the data are shown in Figures 10–12. In the figures, the first bars belong to the neat LDPE, and the second and third bars belong to LDPE/organoclay nanocomposites with 2 wt % clay loading and LDPE/compatibilizer blends with a 5 wt % compatibilizer loading, respectively. The fourth bars indicate the ternary compounds of these materials.

In thermoplastic-based nanocomposites (intercalated or exfoliated), the stress at break value expresses the ultimate strength that the material can bear before break and varies strongly depending on the nature of the interactions between the polymer matrix and the filler.[1] Usually, rigid particulate fillers decrease the tensile strength of a material, unless good adhesion is attained at the interface.[19] Figure 10 shows that addition of 2 wt % of organoclays Cloisite® 25A or Cloisite® 30B to neat polymer decreased the tensile strength of the neat polymer.

It is seen that, with a 5 wt % loading of the compatibilizer, the tensile strength and tensile modulus values of the neat LDPE decrease, because the compatibilizer has lower tensile strength and tensile modulus than LDPE has.

In Figure 10, highly improved tensile strength values are observed for the ternary nanocomposites. Figure 11 shows that the tensile modulus is also highly improved when ternary nanocomposites are formed. The extent of the improvement of the tensile strength and modulus depends upon the goodness of dispersion and the average length of dispersed clay particles. Alignment of clay layers in the direction of injection molding also results in high improvement in the tensile strength and modulus.[20] Another reason for the drastic improvement in tensile strength and modulus in these ternary nanocomposites is the strong interaction between the well-dispersed silicate layers and the matrix, via formation of the bonds between the functional group of the compatibilizer and the hydroxyl groups of the organoclays.[21] In other words, the reactions between the functional groups of the compatibilizer (GMA and MAH), and the groups on the organoclay surface (OH), increase the adhesion of the polymer matrix and the organoclay. Owing to this improvement, the stresses are much more effectively transferred from polymer matrix to the inorganic filler, and thus a high increase in tensile strength and modulus is expected.[22]

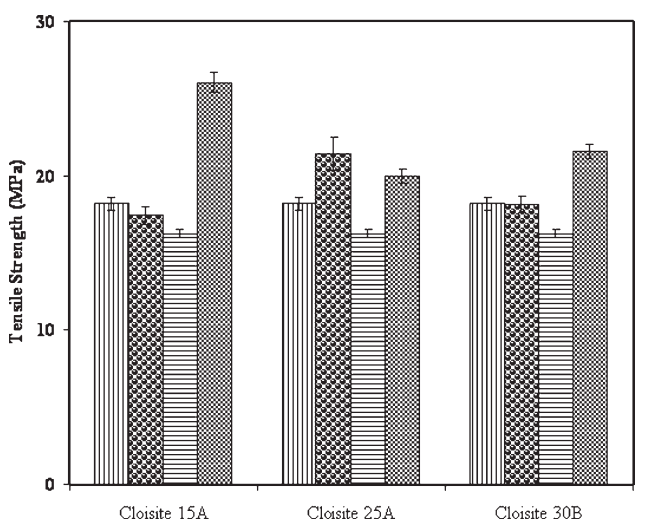

Figure 10 Tensile strength of the materials prepared.

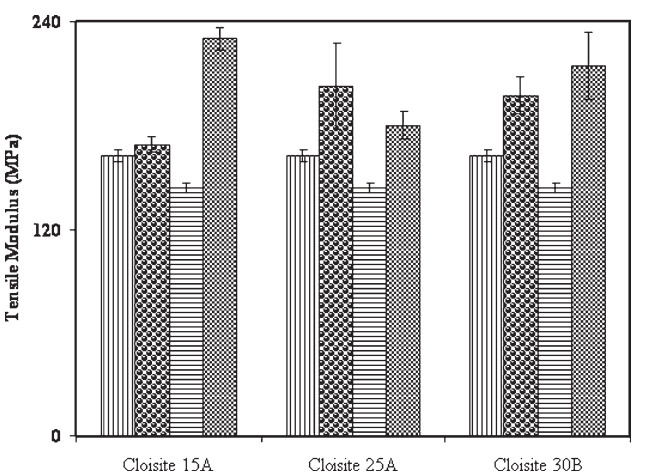

Figure 11 Tensile modulus of the materials prepared.

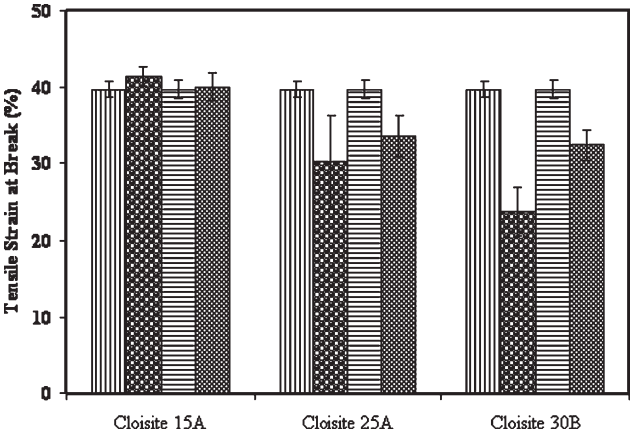

Figure 12 Tensile strain at break of the materials prepared.

When compared with the tensile strength and modulus of binary LDPE/organoclay nanocomposites and ternary LDPE/compatibilizer/organoclay nanocomposites, the latter are characterized by higher strength and modulus increases for the same organoclay loading. These results are expected based on the morphological analysis results described earlier. All the ternary nanocomposites are either intercalated or partially exfoliated.

Among the ternary LDPE/E-MA-GMA/organoclay nanocomposites, the maximum increase in tensile strength and tensile modulus values was observed for the ones prepared with Cloisite® 15A. The improvement with respect to neat LDPE was 43% for tensile strength and 44% for tensile modulus. In the nanocomposites prepared with Cloisite® 30B, improvement in tensile strength and tensile modulus was 18.7 and 32%, respectively. According to the XRD results, Cloisite® 30B-based ternary nanocomposites were nearly totally exfoliated. However, in exfoliated samples, the improvement in tensile strength and tensile modulus is not as high as in intercalated samples, because alignment of the clay layers in the direction of injection molding is more difficult in exfoliated samples. It was observed that, alignment of the clay layers in the direction of injection molding results in the highest improvement in the tensile strength and modulus.[20] The effects of the addition order were studied in Cloisite® 15A-based nanocomposites, because they exhibited the highest improvement in these properties.

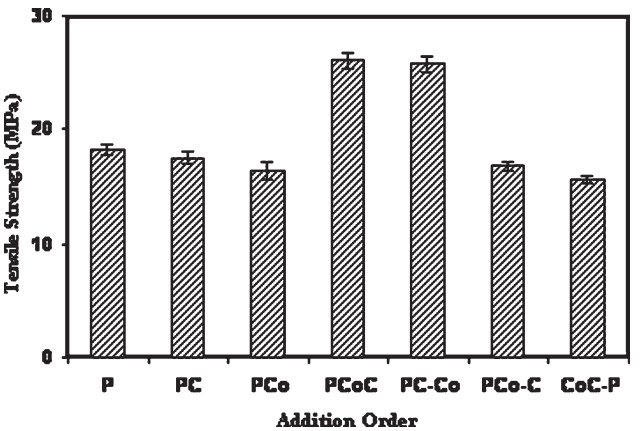

Figure 13 Effect of addition order on the tensile strength of LDPE/E-MA-GMA/Cloisite® 15A nanocomposites containing 5 wt % E-MA-GMA and 2 wt % organoclay.

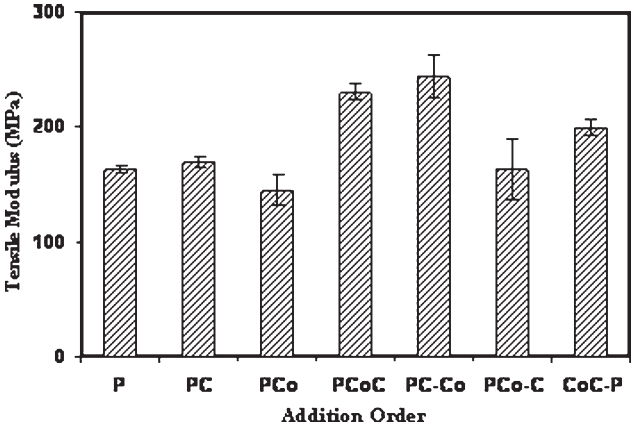

Figure 14 Effect of addition order on the tensile modulus of LDPE/E-MA-GMA/Cloisite® 15A nanocomposites containing 5 wt % E-MA-GMA and 2 wt % Cloisite® 15A.

With an increase of 9.6% in tensile strength and 11% increase in tensile modulus, the lowest improvement was observed in the LDPE/E-MA-GMA/Cloisite® 25A nanocomposites.

Figure 12 shows the tensile strain at break values of LDPE/compatibilizer/organoclay nanocomposites. It is observed that, for the nanocomposites that have the best tensile strength and tensile modulus values, there were no significant changes in the tensile strain at break values. All the materials fractured after yielding. Apparently, the presence of organoclay and/or compatibilizer at these levels does not affect the fracture mechanism.

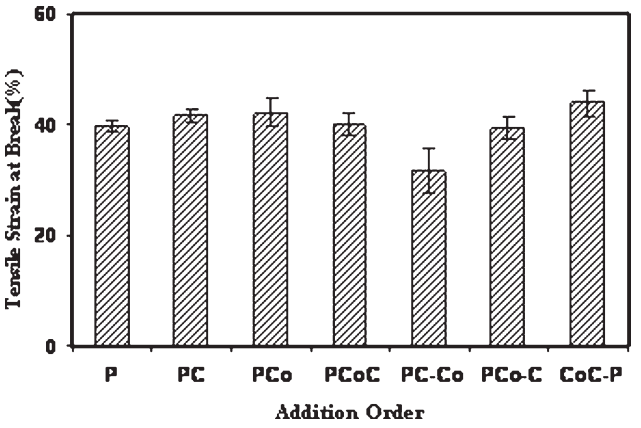

Figure 15 Effect of addition order on the tensile strain at break value of LDPE/E-MA-GMA/Cloisite® 15A nanocomposites containing 5 wt % E-MA-GMA and 2 wt % Cloisite® 15A.

TABLE IV
MFI (g/10 min) Values of Samples Containing 2 wt % Cloisite® 15A, 25A, and 30B with/without 5 wt % Compatibilizer

	No clay	2 wt % Cloisite® 15A	2 wt % Cloisite® 25A	2 wt % Cloisite® 30B
LDPE (not extruded)	1.86	–	–	–
LDPE (twice extruded)	2.84	2.29	2.02	1.89
LDPE/E-MA-GMA	1.57	1.76	1.85	2.05

Figures 13–15 show the mechanical properties of LDPE/E-MA-GMA/Cloisite® 15A nanocomposites produced by the addition order procedures indicated in Table II. Based on the tensile properties, PCoC (AO4) mixing order seems to be the best addition sequence in which all the materials were fed to the extruder in the first run, and the product of the first run was extruded once more. In general, these nanocomposites showed the highest improvement in tensile strength and tensile modulus when compared with nanocomposites prepared with other addition order sequences. In this mixing order, the interactions between the three components are maximized, because they spend the longest time with each other in this procedure. In addition to these, elongation at break behavior of the nanocomposites prepared with the fourth addition order was not poor indicating well dispersion of the silicate layers in the polymer matrix.

Flow properties of nanocomposites

The MFI test was carried out under a specified load of 2.16 kg and temperature of 270°C. Table IV summarizes the MFI values of samples containing 2 wt % Cloisite® 15A, 25A, and 30B with/without 5 wt % E-MA-GMA. The differences in MFI values (g/10 min) were so small that it is difficult to have exact conclusions about the flow properties of the samples. It is seen that MFI of neat LDPE increased (viscosity decreased) after the extrusion processes owing to the decrease in the molecular weight of the LDPE, due to the applied shear during the extrusions. In binary nanocomposites, the addition of organoclay decreased MFI (increased viscosity) in comparison with twice extruded LDPE, as expected. In Table IV, the MFI data are for ternary compositions prepared by the fourth mixing order. Except for the material with Cloisite® 30B, the ternary nanocomposites have lower MFI (higher viscosity) than their binary counterparts, because the viscosity of the compatibilizer is higher than that of LDPE. In the ternary, nanocomposite with Cloisite® 30B slip was observed giving rise to high-effective MFI.

CONCLUSIONS

Ternary nanocomposites of LDPE were produced with different organoclays and an ethylene-based compatibilizer (E-MA-GMA) by means of melt compounding method. Effects of compatibilizer, organoclay, and the addition order of the components, on the morphology, thermal properties, mechanical properties, and flow behavior, were investigated.

According to XRD analysis, intercalation of polymer was observed in LDPE/organoclay binary nanocomposites. Addition of 5 wt % compatibilizer to LDPE/organoclay nanocomposites positively affected the dispersion of the organoclay particles, resulting in shifting of the organoclay peaks to smaller angles. Also, in ternary nanocomposites, the diffraction peaks were broader and lower in height in comparison with those of the neat organoclay and binary LDPE/organoclay nanocomposites. Intercalation and partial exfoliation of the organoclay layers were achieved in the ternary nanocomposites.

SEM micrographs showed that the smooth surface of the pristine LDPE disappeared when melt blended with organoclay. In SEM micrographs of ternary nanocomposites, the smooth structure of neat LDPE was not detected, and many shorter and closer, circular, nonlinear crack propagation lines were the evidence of the well dispersion of the organoclays throughout the matrix. TEM micrographs confirmed that compatibilized polymer matrix had intercalated into the layers of the organoclays.

Addition of organoclay and/or compatibilizer did not influence the melting/crystallization behavior of the nanocomposites. It was concluded that the compatibilizer and organoclay types had no significant nucleation activity in LDPE.

The tensile strength and tensile modulus showed notable improvements in ternary nanocomposites with respect to neat LDPE and binary LDPE/organoclay nanocomposites. LDPE/E-MA-GMA/Cloisite® 15A nanocomposites showed the highest improvement in mechanical properties. Based on tensile properties, the best addition sequence is the one in which all the materials were simultaneously fed to the extruder in the first run, and the product of the first run was extruded once more.

References

1. Alexandre, M.; Dubois, P. Mater Sci Eng 2000, 28, 1.
2. Giannelis, E. P. Adv Mater 1996, 8, 29.
3. Bafna, A. A. Ph. D. Thesis, University of Cincinnati, 2004.
4. Gopakumar, T. G.; Lee, J. A.; Kontopoulou, M.; Parent, J. S. Polymer 2002, 43, 5483.

5. Kato, M.; Okamoto, H.; Hasegawa, N.; Tsukigase A.; Usuki, A. Polym Eng Sci 2003, 43, 1312.
6. Zhai, H.; Xu, W.; Guo.; Zhou, H. Z.; Shen, S.; Song, Q. Eur Polym J 2004, 40, 2539.
7. Zhao, C.; Qin, H.; Gong, F.; Feng, M.; Zhang, Z.; Yang, M. Polym Degrad Stab 2004, 87, 183.
8. Wang, K. H.; Choi, M. H.; Koo, C. M.; Choi, Y. S.; Chung, I. J. Polymer 2001, 42, 9819.
9. Zhang, J.; Wilkie, C. A. Polym Degrad Stab 2003, 80, 163.
10. Liang, G.; Xu, J.; Bao, S.; Xu, W. J Appl Polym Sci 2004, 91, 3974.
11. Hotta, S.; Paul, D. R. Polymer 2004, 45, 7639.
12. Morawiec, J.; Pawlak, A.; Slouf, M.; Galeski, A.; Piorkowska, E.; Krasnikowa, N. Eur Polym J 2005, 41, 1115.
13. Hwang, S.; Hsu, P. P.; Yeh, J.; Chang, K.; Lai, Y. Int Commun Heat Mass Transfer 2009, 36, 471.
14. Yang, H.; Song, Y.; Xu, B.; Zheng, Q. Chem Res Chin Univ 2005, 22, 383.
15. ASTM D638-91a. Annual Book of ASTM Standards 1993, 08.01, 174.
16. Yoon, J. T.; Jo, W. H.; Lee, M. S.; Ko, M. B. Polymer 2001, 42, 329.
17. Dennis, H. R.; Hunter, D. L.; Chang, D.; Kim, S.; White, J. L.; Cho, J. W.; Paul, D. R. Polymer 2001, 42, 9513.
18. Yilmazer, U.; Ozden, G. Polym Compos 2006, 27, 249.
19. Nielsen., L. E.; Landel, R. F. Mechanical Properties of Polymers and Composites; Marcel Decker: New York, 1994.
20. Isik, I.; Yilmazer, U.; Bayram, G. Polym Compos 2008, 29, 133.
21. Ray, S. S.; Okamoto, M. Prog Polym Sci 2003, 28, 1539.
22. Manias, E.; Touny, A.; Wu, L.; Strawhecker K.; Lu, B.; Chung T. C. Chem Mater 2001, 13, 3516.